Control Effect of Flow through Perforated Inlet Diffuser in the Rectangular Settling Tanks. I. Theoretical Considerations

By

Takeshi GODA* and Tomitaro SUEISHI*

(Received January 31, 1961)

In this paper, flow behaviour in the controlled inlet chamber of a rectangular settling tank are analysed two-dimensionally considering the lateral outflow through the perforated diffuser wall, and the effect of flow training or regulation by that type of diffuser are discussed in detail. In the case where the direction of the inflow is parallel to the diffuser wall, the distribution characteristics of the rate of discharge at the outer side of the diffuser seem similar to those for flow through a uniformly perforated pipe, a case which was previously analysed by one of the authors[1], and resulted in a flow with the tendency to turn aside towards the far end of the side wall. When the direction of inflow is perpendicular to the diffuser wall, a circulation of large scale occurs in the inlet zone upstream of the diffuser wall, and the velocity distribution along the diffuser wall shows very delicate changes. These results depend on numerical calculations based on an anylysis in which the viscosity is neglected and some other practical approximations are made.

1. Introduction

One of the important hydraulic principles in designing various facilities for water purification and waste water disposal is that the more uniformly water is distributed or collected to and from all parts of the cross section in the facility, the higher the efficiency of treatment. Any accessory devices equipped with this aid may be defined as "training devices" generally in a wide sense; among them, inlet and outlet perforated or slotted diffuser walls, vertical baffle plates, longitudinal training walls, submerged overflow weirs and overflow troughs used in settling tanks, the underdrain systems and overflow troughs equipped in sand filters are regarded as examples of "training devices" of a popular kind, which are adopted very widely for use in the field. For the problem of regulating flow in a sedimentation basin, the perforated diffuser wall seems to give superior results compared with other kinds of accessories because the flow regulation or control is quite effective not only in the horizontal, but also in the vertical direc-

* Department of Sanitary Engineering

tion. In general, a diffuser wall is built perpendicular to the main flow at the inlet or outlet part of the basin, and in some cases other flow training devices such as a longitudinal training wall or transversal baffle walls are also provided. Furthermore, from time to time, in order to increase the settling efficiency, intermediate diffuser walls are constructed according to the length and width of the basin.

However, all the flow training devices mentioned above are constructed to prevent density currents, shortcircuiting due to wind drift, and disturbances of flow due to sludge deposits which might occur in the main body of water, while for the case where such phenomena are not expected to happen, flow training both at the inlet and outlet zones will usually be sufficient to maintain a favourable volumetric efficiency. In another words, regulation or training of flow at the inlet, in general, is of the most important significance in the design of settling basin.

Many experiments have been performed by using models or actual basins, and the results have been used to determine the most suitable position for the perforated diffuser plate and ratio of perforation. Nevertheless, these results have only a restricted range of validity because most of the experiments were performed under certain special hydraulic conditions and with only a few definite types of apparatus. One of the difficulties in comparing the results of flow regulation by model is the difficulty of measuring the local velocities in the vicinity of the diffuser, though, tracer methods are often used to calculate the volumetric basin efficiency indirectly. However, it is still considered difficult to avoid the undesirable effects due to the density difference between the tracer cloud and water fractions. Conventional design practices used in municipal water works are such that a proper length is selected for the space between the inlet end and the diffuser wall at first, and then slotted with a number of 10 to 15 cm diameter circular or rectangular holes so as to make the percent reducing rate about 5 to 10%. It really seems quite inefficient to have many similar experiments still being made independently for each newly designed plant. Most of the inlet flow control devices designed hitherto are not thought to be permanent, at least in the theoretical sense, but considered as temporary although recently a few up-to-date plants have adopted some new ideas, for example[2),3)], the use of double vertical diffusers with fine and coarse perforations respectively.

It is generally recognized that the perforated diffuser adjusts the irregularity of local energy distribution and results in a considerable dissipation of energy. In order to confirm the basic design criteria for the inlet diffuser on a theoretical basis, this series of papers will discuss the control mechanism of the perforated

type diffuser hydraulically, especially for flow in the vicinity of the diffuser wall, by a two-dimensional analysis of the flow which accompanies lateral inflow and outflow; theories are introduced for a few representative boundary conditions, and the results will be discussed together with some data from model experiments in the next paper.

2. Fundamental Concepts for the Two-Dimensional Analysis of Flow in the Inlet Chamber

Typical arrangements for the inlent perforated diffusers in the inlet zone of a sedimentation basin are shown in Figs. 1 and 2, in which, Fig. 1 signifies the case where the direction of inflow is perpendicular to the longitudinal axis of

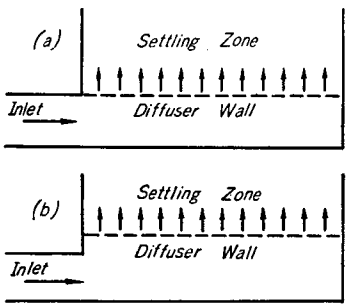

Fig. 1. Inlet channels perpendicular to the basin axis.

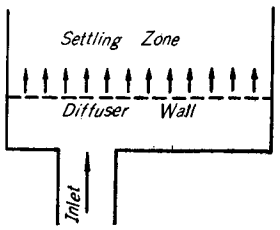

Fig. 2. Inlet channel parallel to the basin axis.

the basin, and Fig. 2 shows the case where the two directions are parallel to each other; a similar classification may be given for the relative vertical position of the inlet conduit to the basin. However, inasmuch as the depth of a basin is generally considerably less than the width, a gradual increase in the vertical velocity gradient is inevitable at the downstream sections even if the vertical training of the flow were completely successful at the upstream section. Therefore, methods must first be found for the training of flow in any horizontal cross section.

From this standpoint, the authors first treat the simplified problem of flow through rectangular sectioned inlet conduits as shown in Figs. 1 and 2, assuming that the bed of the basin is even everywhere.

Another assumption takes the water depth in the sedimentation basin as constant, by reason of the fact that the mean flow velocity in the basin is low enough to be accessible. Therefore, the flow in the inlet zone can be replaced with the hydraulic system of an uniform pressure chamber, in which, any local change in pressure corresponds to a change in depth in the original hydraulic system.

In this paper, the whole channel part in the basin upstream of the diffuser wall is defined as the "inlet chamber".

For the simplicity of mathematical treatment it is necessary to neglect the terms concerned with fluid viscosity in the momentum equation even for the irrotational motion. In such cases, sometimes the method of conformal representation was used to check the velocity potentials and draw streamlines. For example, one of the authors even investigated[4] the relationship between the flow patterns and the shapes of the corners in the grit chamber by this method. However, in actual basins, the observed flow behaviours show a greater variety than expected from the results computed by the above method, i.e., the formation of a large vortex, the superiority of flow along the opposite side wall, the backward current or the appearance of large stagnant zone. These facts probably mean that the mathematical treatment assuming non-vortex motion is improper for such problems though the effects of fluid viscocity may be of little importance practically.

In Fig. 3, the broken line B–B denotes the perforated diffuser wall, x, y are the coordinates and the x-direction corresponds to that of the main flow in the inlet chamber. The velocity components in the x- and y-directions are u and v respectively, so, u represents the local velocity of the main flow. Physical significance of the assumed boundary B–B is defined such that only the positive outflow v_l is admitted in the y-direction through the boundary, although the pressure is transmitted continuously.

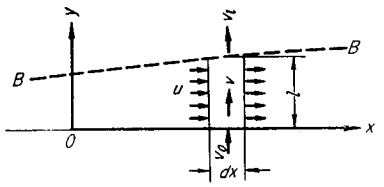

Fig. 3. Two-dimensional flow in the inlet chamber.

Equation of continuity for the two-dimensional flow is written as

$$\frac{\partial u}{\partial x}+\frac{\partial v}{\partial y}=0\,, \tag{1}$$

and its integrated form is written as

$$v_0-v=\int_0^y \frac{\partial u}{\partial x}\,dy\,, \tag{2}$$

for $(v)_{y=0}=v_0$. From the assumption mentioned above, it becomes

$$v_0-v_l=\frac{\partial}{\partial x}(Ul)\,. \tag{3}$$

As U denotes the mean velocity in the x-direction and l the chamber width, Eq. (3) signifies the equation of continuity for the mean flow in the x-direction,

where v_0-v_l is equal to the increase in quantity transported in the y-direction per unit length.

The momentum equation for the x-direction is derived by equating the increase of momentum per length dx, $dx\cdot\partial\left(\int_0^l \rho u^2 dy\right)\Big/\partial x$, with summation of pressure terms, $-dx\cdot\partial\left(\int_0^l p dy\right)\Big/\partial x + dx\cdot p_l\,\partial l/\partial x$. Therefore,

$$\rho\frac{\partial}{\partial x}(\alpha_m U^2 l) = -l\frac{\partial \bar{p}}{\partial x} - (\bar{p}-p_l)\frac{\partial l}{\partial x}, \tag{4}$$

where ρ is the density, $\alpha_m=\int_0^l u^2 dy\Big/U^2 l$, p is the internal pressure, $p_l=(p)_{y=l}$ and $\bar{p}=\int_0^l p dy\Big/l$. The terms of resistance due to viscosity are neglected.

On the other hand, Euler's equation of motion for the two-dimensional steady state flow are given as

$$\begin{aligned} u\frac{\partial u}{\partial x}+v\frac{\partial u}{\partial y} &= -\frac{1}{\rho}\frac{\partial p}{\partial x}, \\ u\frac{\partial v}{\partial x}+v\frac{\partial v}{\partial y} &= -\frac{1}{\rho}\frac{\partial p}{\partial y}. \end{aligned} \tag{5}$$

If u is given, α_m and the local value of v by Eq. (2) are obtained; then $\partial p/\partial y$ is computed by the second equation of (5). Furthermore, $\bar{p}$ is also calculated by p_l which is given as the boundary condition at $y=l$. Thus, the motion in the x-direction is made distinct by solving Eqs. (3) and (4).

The following equation represents the relation of the heads at two points, before and after the flow passes one of the perforated orifices on B–B.

$$\frac{v_i^2}{2g}+\frac{p_l}{\rho g} = f_r\frac{v_d^2}{2g}+\frac{p_i'}{\rho g}, \tag{6}$$

in which g is the gravity acceleration, the first term on the right side means the loss of head through the orifice, p_i' denotes the internal pressure at the exit and v_d is the actual velocity of flow in the perforation that may be expressed as $v_d=v_i/e$, where e is the perforation ratio of the wall B–B. In case a better controlling effect is required, the value of e might bocome considerably less. Therefore, taking the relation $v_i^2 \ll v_d^2$ into account, Eq. (6) can be simplified:

$$\begin{aligned} (p_l-p_i')/\rho g = \varepsilon v_i^2/g = v_i^2/2gc^2e^2, \\ \text{where} \qquad \varepsilon = f_r/2e^2 = 1/2c^2e^2, \end{aligned} \tag{7}$$

and c is generally called the discharge coefficient.

Eqs. (3), (4) and (7) are the fundamental equations for analysing the flow in the inlet chamber.

If the width of the inlet chamber is l uniformly and the length of the diffuser wall is B, then Eqs. (3), (4) and (7) will be solved together using the known value of e, v_0, p_l' and U at $x=0$, B, by which p_l or $\bar{p}$, v_l and U are obtained. By another way, p_l, U and e are regarded as unknowns if v_l is known, and the mathematical treatment becomes somewhat easier and more convenient since p_l and U are obtained by Eqs. (3) and (4) and e, independently, is computed by Eq. (7) thereafter.

One of the requirements for using this theory due to a one-dimensional treatment is that the distribution of u must be given at the initial section and some kind of assumption is made for the actual calculation. For example, assuming that u is uniform at $x=0$ by regarding l as small enough compared with B. This problem will be discussed again later in this paper.

3. Rectangular Inlet Chamber with an Inlet Diffuser adjacent to the Side Wall of Inlet Channel

A rectangular inlet chamber, width l and length B, is considered, and the $x-y$ co-ordinates are taken from the origin 0 at the nearer corner of the chamber as shown in Fig. 4. Raw water is introduced from the inlet channel with an average velocity U_0 at $x=0$, so, v_0 equals zero at the initial section. Eqs. (3) and (4) are written simply as

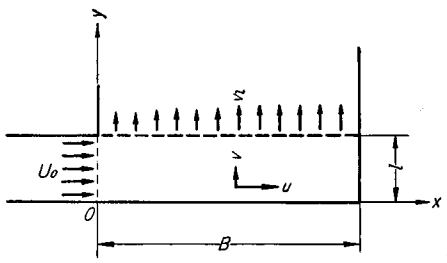

Fig. 4. Rectangular inlet chamber with an inlet diffuser adjacent to the side wall of inlet.

$$\frac{dU}{dx} = -\frac{v_l}{l} \tag{8}$$

and

$$\frac{d}{dx}\left(\frac{\alpha_m U^2}{g}\right) = -\frac{1}{\rho g}\frac{d\bar{p}}{dx}, \tag{9}$$

respectively. The third equation required in this case is considered to be the same as Eq. (7) in form, therefore, integration of Eqs. (8) and (9) make

$$U = \frac{1}{l}\int_x^B v_l dx \tag{10}$$

and

$$\frac{\alpha_m U^2}{g} = \frac{\bar{p}_B}{\rho g} - \frac{\bar{p}}{\rho g}, \tag{11}$$

while $(U)_{x=B}=0$ and $(\bar{p})_{x=B}=\bar{p}_B$.

On the other hand, the second equation of (5) is transformed by substituting Eq. (1) in it to yield

$$\frac{u^2}{g}\frac{\partial}{\partial x}\left(\frac{v}{u}\right)=-\frac{1}{\rho g}\frac{\partial p}{\partial y}. \tag{12}$$

As assumed above, the value of v/u becomes zero at $y=0$ and $v_l/(u)_{y=l}=v_l/u_l$ at $y=l$. Therefore if a linear change of v/u may be assumed between $y=0$ and l,

$$\frac{v}{u}=\frac{v_l}{u_l}\frac{y}{l}, \tag{13}$$

and accordingly, Eq. (12) becomes

$$\frac{u^2}{g}\frac{y}{l}\left(\frac{1}{u_l}\frac{dv_l}{dx}-\frac{v_l}{u_l^2}\frac{du_l}{dx}\right)=-\frac{1}{\rho g}\frac{\partial p}{\partial y}. \tag{14}$$

For simplicity, $\alpha_m U^2$ is used instead of u^2 and also a finite value σ is introduced as $u_l=\sigma U$, then, the integration of Eq. (14) for y to l reduces to the relationship

$$\frac{p}{\rho g}=\frac{p_l}{\rho g}+\frac{\alpha_m}{2g\sigma l}\left(U\frac{dv_l}{dx}-v_l\frac{dU}{dx}\right)(l^2-y^2), \tag{15}$$

by which, the distribution of pressure head in the transversal direction y can be calculated.

To calculate $\bar{p}$, Eq. (15) is integrated from 0 to l with respect to y and Eqs. (8), (10) are substituted in it to yield

$$\frac{\bar{p}}{\rho g}=\frac{p_l}{\rho g}+\frac{\alpha_m}{3g\sigma}\left(\frac{dv_l}{dx}\int_x^B v_l dx+v_l^2\right), \tag{16}$$

and especially for $\bar{p}_B$ ($\bar{p}$ at $x=B$), it becomes

$$\frac{\bar{p}_B}{\rho g}=\frac{p_{l,B}}{\rho g}+\frac{\alpha_m}{3g\sigma}v_{l,B}^2, \tag{16}'$$

where $p_{l,B}=(p_l)_{x=B}$ and $v_{l,B}=(v_l)_{x=B}$.

Another form of differential equation is obtained by substituting Eqs. (10), (16) and (16)′ into Eq. (11).

$$\frac{p_l}{\rho g}+\frac{\alpha_m}{3g\sigma}\left(\frac{dv_l}{dx}\int_x^B v_l dx+v_l^2\right)=\frac{p_{l,B}}{\rho g}+\frac{\alpha_m}{3g\sigma}v_{l,B}^2-\frac{\alpha_m}{g}\left(\frac{1}{l}\int_x^B v_l dx\right)^2. \tag{17}$$

For the convenience of mathematical treatment and physical significance, another notation Y is used to represent the difference in pressure head between the point at x in the inlet chamber and that just outside the diffuser, which is defined as

$$(p-p_l')/\rho g=Y \tag{18}$$

and the same suffixes as for p are used for Y. In the open channel system, Y corresponds to the decrease in water level just outside of the diffuser wall.

Assuming that p_l'=constant may be necessary for the simplest case in which only the direct effect of the diffuser is discussed, and furthermore, since it may also be allowed even for the general case in which the trained effects of flow are discussed in detail, the mathematical treatment is greatly simplified. Eqs. (7) and (17) are transformed to

$$Y_l = \varepsilon v_l^2/g \tag{19}$$

and
$$Y_l + \frac{\alpha_m}{3g\sigma}\left(\frac{dv_l}{dx}\int_x^B v_l dx + v_l^2\right) = Y_{l,B} + \frac{\alpha_m}{3g\sigma}v_{l,B}^2 - \frac{\alpha_m}{g}\left(\frac{1}{l}\int_x^B v_l dx\right)^2 . \tag{20}$$

With Eqs. (19) and (20), Y_l is diminished and a new differential equation concerning v_l is introduced:

$$\alpha_m\left(\int_x^B v_l dx\right)^2 + \frac{\alpha_m l^2}{3\sigma}\frac{dv_l}{dx}\int_x^B v_l dx + l^2\left(\frac{\alpha_m}{3\sigma}+\varepsilon\right)(v_l^2 - v_{l,B}^2) = 0 . \tag{21}$$

Here, a dimensionless variable r related to v_l is defined as

$$v_l B \Big/ \int_0^B v_l dx = v_l B/U_0 l = r , \tag{22}$$

and the same suffixes are used for r as for v_l. Furthermore, two other dimensionless factors, λ and ξ, are introduced thereafter:

$$l/B = \lambda , \qquad x/B = \xi . \tag{23}$$

Using r, λ and ξ, Eq. (21) becomes non-dimensional.

$$\alpha_m\left(\int_\xi^1 r d\xi\right)^2 + \frac{\alpha_m\lambda^2}{3\sigma}\frac{dr}{d\xi}\int_\xi^1 r d\xi + \lambda^2\left(\frac{\alpha_m}{3\sigma}+\varepsilon\right)(r^2 - r_B^2) . \tag{24}$$

Eq. (24) is the simplified form of a differential equation which must be solved for v_l; first of all, the most ordinary case where ε is constant will be discussed.

A replacing factor

$$\int_\xi^1 r d\xi = s$$

is used in Eq. (24), which is integrated once with respect to ξ, and then takes the form

$$r = -\frac{ds}{d\xi} = \sqrt{Cs^{(2+6\sigma\varepsilon/\alpha_m)} - \frac{\alpha_m s^2}{\lambda^2\varepsilon} + r_B^2} , \tag{25}$$

where C is the integration constant. The process of determining C is as follows. As previously assumed, the velocity distribution at $x=0$ is uniformly U_0, the internal pressure must also be uniform at $x=0$ and should vary continuously, from Eqs. (8), (12) and (13)

$$\begin{aligned} (dv_l/dx)_{x=0} &= -v_{l,0}^2/U_0 l , \qquad \text{where} \qquad v_{l,0} = (v_l)_{x=0} \\ \text{or} \qquad (dr/d\xi)_{\xi=0} &= -r_0^2 \end{aligned} \tag{26}$$

is derived. Since $s=1$ at $\xi=0$, from Eq. (25)

$$\begin{aligned} r_0^2 &= C-\alpha_m/\lambda^2\varepsilon+r_B^2, \\ (dr/d\xi)_{\xi=0} &= -(1+3\sigma\varepsilon/\alpha_m)C+\alpha_m/\lambda^2\varepsilon \end{aligned} \tag{27}$$

are obtained. Furthermore, by subsititution of Eqs. (27) to Eq. (26), and rearrangement, C is found as

$$C = \alpha_m r_B^2/3\sigma\varepsilon\,. \tag{28}$$

Finally, Eq. (25) takes the form

$$r = -\frac{ds}{d\xi} = \sqrt{\frac{\alpha_m s^2}{3\varepsilon}\left(\frac{r_B^2}{\sigma}s^{6\sigma\varepsilon/\alpha_m}-\frac{3}{\lambda^2}\right)+r_B^2}\quad . \tag{29}$$

The value of $r_B^2 s^{6\sigma\varepsilon/\alpha_m}/\sigma$ in Eq. (29) is sufficiently small compared with $3/\lambda^2$ if $\lambda(=l/B)$ is small. On the other hand, even for the larger values of λ, it is recognized that generally the value of e, the perforation ratio, will be taken considerably smaller in order to make ε larger and to increase the effects of controlling flow, so that $s^{6\sigma\varepsilon/\alpha_m}$ becomes a sufficiently small value considering $s<1$ for $\xi>0$. Consequently in most cases, the term $r_B^2 s^{6\sigma\varepsilon/\alpha_m}/\sigma$ can be ignored, which seems equivalent to taking the constant C in Eq. (25) as zero. In this view, Eq. (29) becomes

$$-d\xi = ds\Big/\sqrt{r_B^2-\frac{\alpha_m s^2}{\lambda^2\varepsilon}}, \tag{30}$$

and its solution is reduced easily as follows:

$$\begin{aligned} s &= \lambda\sqrt{\frac{\varepsilon}{\alpha_m}}\,r_B \sin\left\{\frac{1}{\lambda}\sqrt{\frac{\alpha_m}{\varepsilon}}\,(C'-\xi)\right\}, \\ \therefore\quad r &= -\frac{ds}{d\xi} = r_B\cos\left\{\frac{1}{\lambda}\sqrt{\frac{\alpha_m}{\varepsilon}}\,(C'-\xi)\right\}, \end{aligned} \tag{31}$$

where, C' is the integration constant. However, from $C'=1$, $r=r_B$ for $\xi=1$

$$r = r_B\cos\left\{\frac{1}{\lambda}\sqrt{\frac{\alpha_m}{\varepsilon}}(1-\xi)\right\} \tag{32}$$

is derived. Furthermore, referring the first equation of (31) to the condition $s=1$ when $\xi=0$, r_B is determined as

$$r_B = \frac{1}{\lambda}\sqrt{\frac{\alpha_m}{\varepsilon}}\Big/\sin\frac{1}{\lambda}\sqrt{\frac{\alpha_m}{\varepsilon}}\,. \tag{33}$$

Therefore, the final form of r can be written regardless of σ

$$\begin{aligned} r &= \frac{1}{\lambda}\sqrt{\frac{\alpha_m}{\varepsilon}}\cos\left\{\frac{1}{\lambda}\sqrt{\frac{\alpha_m}{\varepsilon}}(1-\xi)\right\}\Big/\sin\frac{1}{\lambda}\sqrt{\frac{\alpha_m}{\varepsilon}} \\ \text{or}\quad r &= \frac{\sqrt{2\alpha_m ce}}{\lambda}\cos\left\{\frac{\sqrt{2\alpha_m ce}}{\lambda}(1-\xi)\right\}\Big/\sin\frac{\sqrt{2\alpha_m ce}}{\lambda}\,. \end{aligned} \tag{34}$$

According to the theoretically reduced formula[1] for a frictionless flow in a pipe, length L, with a blind end and a continuous lateral outflow discharge along the uniform side slit or perforations, the ratio of the outflow rate at any section to the average, r', is given by Eqs. (35) if the pressure outside of the pipe is kept constant.

$$\begin{aligned} &x_c/L = 1-\pi/2\sqrt{2\alpha_m}\,\beta \leqq 0\,, \\ &\qquad r' = \sqrt{2\alpha_m}\,\beta \cos\left\{\sqrt{2\alpha_m}\,\beta\left(1-\frac{x}{L}\right)\right\}\Big/\sin\sqrt{2\alpha_m}\,\beta\,, \\ &x_c/L \geqq 0\,, \\ &\qquad r' = 0 \qquad \text{for} \quad 0 \leqq x \leqq x_c\,, \\ &\qquad r' = \sqrt{2\alpha_m}\,\beta \cos\left\{\sqrt{2\alpha_m}\,\beta\left(1-\frac{x}{L}\right)\right\} \qquad \text{for} \quad x_c \leqq x \leqq L\,. \end{aligned} \tag{35}$$

In the process of reducing the above formulas, the acceleration velocity in the direction perpendicular to the pipe axis was neglected, and β, the ratio of the total effective perforation area to the whole section A, is taken as

$$\beta = caL/SA\,, \tag{35}'$$

where c is the discharge coefficient for each perforation with equal area, a, being spaced uniformly at distance S from each other.

Now, the value of β in the present case is computed as

$$\beta = ceBH/lH = ce/\lambda\,,$$

where H denotes the height of the inlet chamber when replaced by a pressured chamber. Therefore it is proved that Eqs. (34) coincides with the first equation of (35); from this result, it is suggested that the general solution of Eq. (30) may take a similar form, in which the solution for the particular case is added, as Eqs. (35), that is

$$\begin{aligned} &\xi_c = 1-\pi\lambda/2\sqrt{2\alpha_m}\,ce \leqq 0\,, \\ &\qquad r = \frac{\sqrt{2\alpha_m}\,ce}{\lambda}\cos\left\{\frac{\sqrt{2\alpha_m}\,ce}{\lambda}(1-\xi)\right\}\Big/\sin\frac{\sqrt{2\alpha_m}\,ce}{\lambda}\,, \\ &\xi_c \geqq 0\,, \\ &\qquad r = 0 \qquad \text{for} \quad 0 \leqq \xi \leqq \xi_c\,, \\ &\qquad r = \frac{\sqrt{2\alpha_m}\,ce}{\lambda}\cos\left\{\frac{\sqrt{2\alpha_m}\,ce}{\lambda}(1-\xi)\right\} \qquad \text{for} \quad \xi_c \leqq \xi \leqq 1\,. \end{aligned} \tag{36}$$

It is realized from Eqs. (36) that r becomes larger when ξ increases, and particularly, that a part of $r=0$ is produced between the region $0 \leqq \xi \leqq \xi_c$ when ξ_c is larger than zero or $ce/\lambda > \pi/2\sqrt{2\alpha_m}$, so that the value of r increases further due to the increase of ξ in the chamber. These facts suggest that the controlling effect will improve if r everywhere approaches unity for larger values of λ

or smaller values of ce.

To solve Eq. (25) by regarding C as zero is to ignore v, the velocity in y-direction, and its acceleration in the inlet chamber, and for the cases where λ is less as stated previously, v is negligible compared with u, for which the significance of the term $3/\lambda^2$ in Eq. (29) is supported to be closely related.

If the value of λ increases to some degree, Eq. (29) must be solved instead of Eq. (30). However, since r gets closer to unity with larger λ, while the domain in which the values of $s=\int_{\xi}^{1} r d\xi$ approach unity is restricted to an extremely small part in the vicinity of the entrance ($\xi=0$), the term $r_B^2 s^{6\sigma\varepsilon/\alpha_m}/\sigma$ in Eq. (29) might still be practically neglected except for the above mentioned small region. If ε gets even larger, then Eqs. (36) will be applicable for a wider range of ξ; on the other hand, in case ε is rather small, even for larger λ, the applicable range of Eqs. (36) will naturally be restricted to a fairly narrow one. For such cases, r_B must be assumed at first, and the computation made from the start where $\xi=1$ and $s=0$, to a proper range at which $r_B^2 s^{6\sigma\varepsilon/\alpha_m}/\sigma$ can be neglected for $3/\lambda^2$ in order to obtain r and s by Eq. (32); next, by numerical integration of Eq. (29), the condition $s=1$ at $\xi=0$ has to be satisfied. Another method, using a new relationship derived from Eqs. (27) and (28)

$$r_0^2 = r_B^2(1+\alpha_m/3\sigma\varepsilon) - \alpha_m/\lambda^2\varepsilon\,, \tag{37}$$

to obtain the value r_0 for a given r_B, and start the integration from the point $\xi=0$, $s=1$, is also preferable.

By transforming Eq. (16), it becomes

$$\overline{Y} - Y_l = \frac{\alpha_m}{3g\sigma} U_0^2\lambda^2\left(r^2 + s\frac{dr}{d\xi}\right). \tag{38}$$

Now, for the domain in which Eq. (30) is approximately preferable, Eq. (38) is simplified by referring to Eq. (32) as

$$\overline{Y} - Y_l = \frac{\alpha_m}{3g\sigma} U_0^2\lambda^2 r_B^2\,, \tag{38}'$$

which means the difference between $\overline{Y}$ and Y_l is constant. Under such conditions it is recommended that $p_l/\rho g$ or Y_l, which controls v_l directly, be used in Eq. (11) instead of $\bar{p}/\rho g$ or $\overline{Y}$ and naturally, the same solution will be obtained as for the case which ignores the change of Y in the y-direction. Furthermore, from these facts it is made clear that the shape of the water surface in the y-direction is quite the same all over with only changes in its height, for the parts in which Eqs. (30), (32) and (36) are approximately true. On the other hand, if Eq. (29) is applicable Eq. (38) takes on a different form.

$$\overline{Y}-Y_l=\frac{\alpha_m}{3g\sigma}U_0^2\lambda^2r_B^2\{1-s^{(2+6\sigma^2/\alpha_m)}\}\,. \qquad (38)''$$

However, while s gets smaller as ξ increases, Eq. (38)″ approaches to Eq. (38)′. The shape of the water surface, which is assumed as level at $\xi=0$, changes itself gradually to the above described form after the flow entered the inlet chamber. Eq. (29) appears to be applicable for this transition region, though the range of this region is not clear or definite since it is related to the accuracy in computing the value of r. As seen in Eq. (38)′, the lateral velocity distribution becomes uniform as r_B approaches unity, and also, $\overline{Y}-Y_l$ decreases as λ decreases. Accordingly these factors are considered as those which reduce the area of the transition zone.

Fig. 5 shows the variation of r relative to the factors λ and e referring to Eqs. (36), which are examples of cases of neglecting the transition zone due to the comparatively low values of ce. However, for instance in the case where the value of ξ_c becomes 0.320, which corresponds to $\lambda=0.1$, $e=20\%$ in Fig. 6 (a), there seems to be no significant effect due to the diffuser wall between $0\leqq\xi\leqq0.3$, and in such a state the main flow in the sedimentation basin is supposed to turn extremely aside to the opposite side wall, and probably, the distribution of

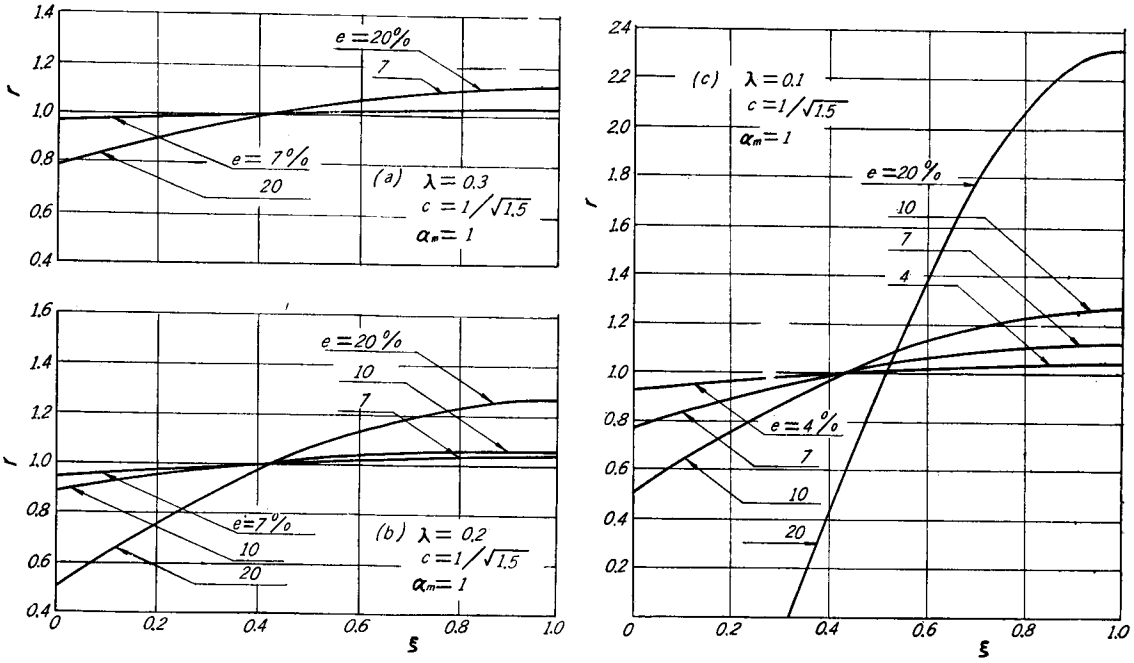

Fig. 5. Flow distributions through diffuser wall with constant perforation ratios (referring to Fig. 4).

pressure just outside of the diffuser wall, p_l', may not uniform as assumed in the former analysis, but actually will strengthen this tendency further.

Fig. 6 shows an example of a numerical calculation for the transitional change of r by Eq. (29), in which the results is compared with that computed from Eqs. (36). It is seen that $r_B=1.922$ and $r_0=0.062$ are obtained due to the existence of the transition zone,

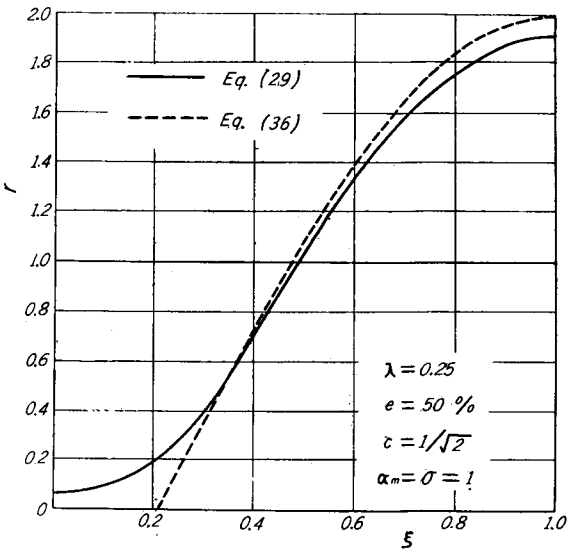

Fig. 6. Flow distribution in the transition region.

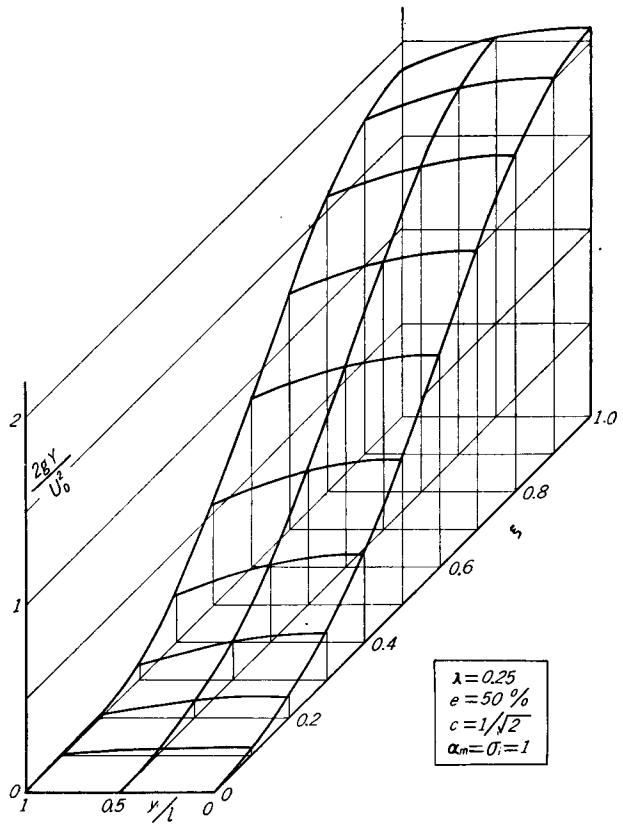

Fig. 7. Transitional change of surface profile.

whereas $r_B=2.000$ and $(r)_{\xi=0\sim0.215}=0$ when the acceleration of v is ignored, so that the effect of the flow regulation seems incresed to some degree. For the example shown in Fig. 6, the range between $\xi=0$ and 0.5 may be recognized as the transition region.

After the dimensionless factor r which is related to v_l is given by the above described methods, Y_l is calculated by a new formula, which is a transformed equation of Eq. (19) referring to Eqs. (22) and (23),

$$Y_l = \frac{\varepsilon\lambda^2 r^2 U_0^2}{g}, \tag{39}$$

then, for Y, calculation will be made according to another new expression

$$Y = Y_l + \frac{\alpha_m \lambda^2 U_0^2}{2g\sigma}\left(r^2 + s\frac{dr}{d\xi}\right)\left\{1-\left(\frac{y}{l}\right)^2\right\}, \tag{40}$$

which was obtained from Eq. (15) in the same manner.

With Eqs. (39) and (40) the variation of Y in the y-direction were calculated for the same conditions as in Fig. 6, and the results are shown in Fig. 7.

It seems difficult from the discussion hitherto made to expect a uniformly controlled velocity distribution by means of an uniformly perforated diffuser wall, and so the tenency of flow to turn more or less aside towards the opposite side wall seems inevitable. Therefore, to secure the ideal condition for velocity distribution, that is, $v_l=$constant, at the inlet section of the basin, changes in the width of the inlet chamber, l, and in the local perforation ratio of the diffuser must be considered.

If the shape of the inlet chamber is rectangular and changing the local ratio of perforation of the diffuser is possible, the following theory is considered applicable. Firstly, the equation of continuity (10) is substituted into Eq. (11) which upon using the notations of r and s again leads to

$$\frac{\alpha_m U_0^2 s^2}{g} = \overline{Y}_B - \overline{Y}. \tag{41}$$

Since making v_l uniform is equivalent to $r\equiv1$, and s must be equal to $1-\xi$. Also Eq. (38), under the conditions $r=1$ and $dr/d\xi=0$, takes the form

$$\overline{Y} = Y_l + \frac{\alpha_m \lambda^2 U_0^2}{3g\sigma}.$$

Furthermore, Eq. (19) is rewritten as

$$Y_l = \lambda^2 r^2 U_0^2/2gc^2e^2.$$

Therefore, by the substitution of these relations into Eq. (41), a finite value of the perforation ratio e^* which makes v_l uniform is given by the following formula.

$$e^* = \frac{\lambda e_B^*}{\sqrt{\lambda^2 - 2\alpha_m c^2 e_B^{*2}(1-\xi)^2}}, \tag{42}$$

where e_B^* denotes the value of e^* at $x=B$.

The required rate of perforation which satisfies the condition $r=1$ at any point is generally obtained by Eq. (42), using the given values of e_B^*, λ and c, and it is easily recognized that e^* must be larger as the point approaches nearer to $x=0$. The maximum possible value of e^* is theoretically unity, but with respect to actual practice, by using the condition $e^* \leqq e_{\max}^*$ at $\xi=0$, the following relation may be introduced.

$$e_B^{*2} \leqq \frac{\lambda^2 e_{\max}^{*2}}{\lambda^2 + 2\alpha_m c^2 e_{\max}^{*2}}. \tag{43}$$

Since l is not very large, usually the relationship $\lambda^2 \ll e_{\max}^{*2}$ is valid and Eq. (43) may be approximated as

$$e_B^{*2} < \frac{\lambda^2}{2\alpha_m c^2}. \tag{43}'$$

Examples of numerical calculations for e^* with regards to Eq. (42) are shown in Fig. 8, in which it is understood that the value of e^* must increase more rapidly towards the entrance section of the inlet chamber for larger values of e_B^* and smaller values of λ.

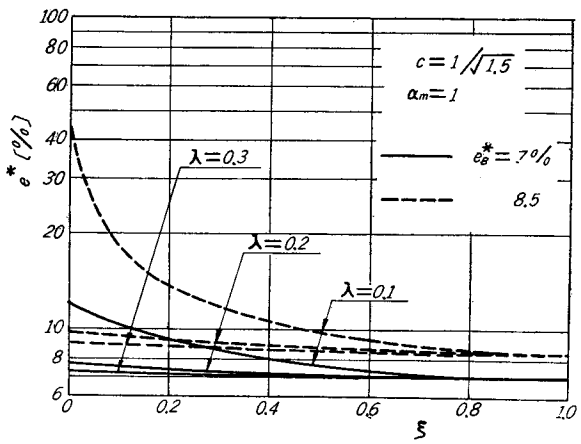

Fig. 8. Necessary change in opening ratio (referring to Fig. 4).

It must be noted, however, that as a necessary condition for applying Eq. (40) the flow in the inlet chamber should satisfy the following relationship

$$Y = Y_l + \frac{\alpha_m \lambda^2 U_0^2}{2g\sigma}\left\{1 - \left(\frac{y}{l}\right)^2\right\}, \tag{44}$$

which is obtained by substituting $r=1$ and $dr/d\xi=0$ into Eq. (40), but it is con-

sidered impossible to satisfy the condition $\partial Y/\partial y=0$, at $\xi=0$. Consequently, it may be concluded that the actual behaviour of flow in the inlet conduit is also being effected by that in the inlet chamber, and gradually changes its characteristic of pressure distribution so as to satisfy Eq. (44), passing through the region of transition after it flowed into the inlet chamber.

4. Rectangular Inlet Chamber with an Inlet Channel Perpendicular to the Diffuser Wall

There are many examples of sedimentation basins so constructed that the axis of the inlet channel is perpendicular to the diffuser; particularly in most cases where the inlets have circular sections. The problem is treated two-dimensionally, and it is assumed that the sectional shape of the inlet conduit is rectangular, with its bottom at the same level as the inlet chamber. Furthermore, for the sake of simplicity, mathematical treatment is applied only to the case in which the inlet is shifted aside relatively to one end as shown in Fig. 9. The same figure will be used in the analysis also for the case where the center line of the inlet conduit coincides with that of the basin, and even for the case where the center line is shifted arbitrarily, the same shaped region may still be considered since it is possible to divide the chamber into two parts in proportion to the properly assumed discharge distribution ratio for the two sides.

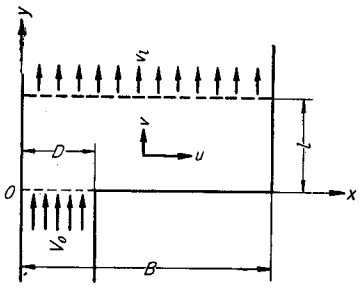

Fig. 9. Rectangular inlet chamber with an inlet perpendicular to the diffuser wall.

Let B and l represnt the length and width of the chamber respectively in the same manner as stated in **3.** and take the $x-y$ co-ordinates as shown in Fig. 9. Water enters the chamber from the inlet opening situated at the reach $x=0$ to D with uniform velocity V_0, the main flow is supposed to be in the x-direction with a lateral inflow rate V_0 and outflow rate v_l per unit length. However, due to considerations of the variations of v and p at the two sides of the section at $x=D$, it is supposed that v does not vary smoothly from $y=0$ to l along the section and may exceed V_0 once in the zone $x<D$, and that u may take a negative sign at the opposite side of the diffuser wall; therefore, a part of the water reaching near the diffuser wall flows back to the inlet by circulation. To explain such a phenomenon as simply as possible, a concept of the supposed "counter flow zone", which spreads over the whole length of the inlet chamber along the wall from $y=0$ to $y=f$, is introduced.

Also, the remaining part, the zone from $y=f$ to l, is named the "regular flow zone", which is distinguished by using the suffix "2" for each notation while the former takes "1". For the convenience of explanation, when necessary, the suffixes "i" and "d" are used for the zones $x=0$ to D and D to B, namely "inlet" and "distributing", respectively. These are shown in Fig. 10.

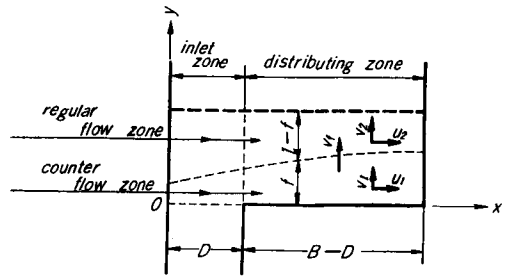

Fig. 10. Supposed divisions of inlet chamber.

The main flows of counter and regular flow zones are considered in the x-direction, and the former has a lateral inflow rate of v_0 and outflow v_f, which denotes v on the boundary of both zones, and the latter, inflow v_f and outflow v_l. Then, the fundamental equations derived in **2.** are again applied to the flows in each zone. From Eqs. (3) and (4), the equations of continuity and equations of motion can be written as follows:

Eqs. of continuity:

$$v_0-v_f=\frac{d(U_1f)}{dx},\qquad v_f-v_l=\frac{d\{U_2(l-f)\}}{dx}, \tag{45}$$

Eqs. of motion:

$$\rho\frac{d(\alpha_mU_1^2f)}{dx}=-f\frac{d\bar{p}_1}{dx}-(\bar{p}_1-p_f)\frac{df}{dx},\qquad \rho\frac{d\{\alpha_mU_2^2(l-f)\}}{dx}=-(l-f)\frac{d\bar{p}_2}{dx}+(\bar{p}_2-p_f)\frac{df}{dx}, \tag{46}$$

where $p_f=(p)_{y=f}$ and $\alpha_{m,1}$ and $\alpha_{m,2}$ are noted together conveniently as α_m. Eq. (12) can be used again in calculating $\bar{p}_1$ and $\bar{p}_2$. Integration of Eq. (12) with respect to y, for $p=p_f$ at $y=f$, gives

$$\int_y^f\frac{u_1^2}{g}\frac{\partial(v_1/u_1)}{\partial x}dy=\frac{1}{\rho g}(p_1-p_f),\qquad \int_f^y\frac{u_2^2}{g}\frac{\partial(v_2/u_2)}{\partial x}dy=\frac{1}{\rho g}(p_f-p_2). \tag{47}$$

Replacing y with l in the second equation of (47) gives the relation between p_l and p_f.

$$\int_f^l\frac{u_2^2}{g}\frac{\partial(v_2/u_2)}{\partial x}dy=\frac{1}{\rho g}(p_f-p_l). \tag{48}$$

Eqs. (47) are integrated once again and if the terms v_1/u_1 and v_2/u_2 are expressed with U_1, v_0 and v_f, and U_2, v_f and v_l respectively, $\bar{p}_1$ and $\bar{p}_2$ are determined from

the difference value of p_f in the next equations.

$$\begin{aligned}\frac{1}{f}\int_0^f dy\int_y^f \frac{u_1^2}{g}\frac{\partial(v_1/u_1)}{\partial x}\,dy &= \frac{1}{\rho g}(\bar{p}_1-p_f),\\ \frac{1}{l-f}\int_f^l dy\int_f^y \frac{u_2^2}{g}\frac{\partial(v_2/u_2)}{\partial x}\,dy &= \frac{1}{\rho g}(p_f-\bar{p}_2).\end{aligned} \tag{49}$$

As the third equation of the three necessary, the discharge equation (7) is applicable for the zone of regular flow; but for the zone of counter flow, the following relation must hold true because of the continuity of values $\partial p_1/\partial y$ and $\partial p_2/\partial y$ at $y=f$.

$$\left\{\frac{u_1^2}{g}\frac{\partial(v_1/u_1)}{\partial x}\right\}_{y=f} = \left\{\frac{u_2^2}{g}\frac{\partial(v_2/u_2)}{\partial x}\right\}_{y=f}. \tag{50}$$

Therefore, by solving the nine equations numbered (45), (46), (48), (49), (7) and (50) simultaneously, the values of v_l, v_f, U_1, U_2, $\bar{p}_1$, $\bar{p}_2$, p_f, p_l and f are obtained as functions of x if e or ε, together with p_l' and v_0 are given.

However, it seems so difficult to take account of Eq. (50) in the process of one-dimensional analysis that, with the concept of inserting an imaginary vertical curtain, through which the flow passes freely in the y-direction but never in the x-direction, as the boundary of both the counter and regular flow zones the condition of Eq. (50) may be avoided. The flow pattern in the chamber is somewhat distorted due to this imaginary curtain, but there must be a value of f which corresponds to the least distortion of flow. The deficiency of a number of equations due to the failure to use Eq. (50) can be filled by an appropriate boundary condition. For the case of Fig. 9, as the value of v_0 is equal to V_0 in the inlet zone, whereas $v_0=0$ in the distributing zone, the solutions must be obtained independently for each zone and after that they will be succesfully connected by the next two conditions at $x=D$ if analysed one-dimensionally.

$$(U_{1,i})_{x=D} = (U_{1,d})_{x=D} \quad \text{and} \quad (U_{2,i})_{x=D} = (U_{2,d})_{x=D}, \tag{51}$$

$$(\bar{p}_{1,i})_{x=D} = (\bar{p}_{1,d})_{x=D} \quad \text{and} \quad (\bar{p}_{2,i})_{x=D} = (\bar{p}_{2,d})_{x=D}. \tag{52}$$

The distribution characteristic of p_i may differ considerably from that of p_d in relation to the value of f even if $\bar{p}_1$ and $\bar{p}_2$ satisfied Eqs. (52). Therefore, it is necessary that the following condition should also be satisfied.

$$(p_{1,i})_{x=D} = (p_{1,d})_{x=D} \quad \text{and} \quad (p_{2,i})_{x=D} = (p_{2,d})_{x=D}. \tag{53}$$

Eq. (53) serves to yield the value of f instead of Eq. (50). If a functional relationship between f and x is assumed and it is only necessary to find the value of f at a definite section, then Eq. (53) is not always necessarily satisfied but the condition of Eq. (54) is preferred practically, by which p_i and p_d will be

made approximately equal at the boundary :

$$(p_{f,i})_{x=D} \cong (p_{f,d})_{x=D} . \tag{54}$$

Analysing that condition of flow in the inlet chamber is a problem of boundary values, so the solutions are usually obtained by the method of numerical integration with the given boundary conditions. However, it is supposed very difficult to satisfy the boundary conditions at $x=0$ and B without repeated calculations. Therefore, in the following treatment it is assumed convenience that f is constant and that u_1, u_2 are uniform in the y-direction, although the accuracy of the approximation will probably be lowered. Also, the ideal case in which v_l is constant is imagined in order to analyse the flow pattern in the zones and to decide the required changing rate of the openings, e^* or ε^*. The merit of this treatment is that the mathematical processes may be greatly simplified, and yet, it seems possible from the results to assume that the distribution of v_l in case e or ε is constant.

Now, for the flow in the inlet zone $(0 \leqq x \leqq D)$, the equations of continuity (45) take the form,

$$\frac{dU_1}{dx} = \frac{V_0 - v_f}{f} \quad \text{and} \quad \frac{dU_2}{dx} = \frac{v_f - v_l}{l-f} . \tag{55}$$

Since $u_1 = U_1$ and $u_2 = U_2$, substituting Eqs. (55) into Eq. (2) makes

$$v_1 = V_0 - (V_0 - v_f)\frac{y}{f} \quad \text{and} \quad v_2 = \frac{v_f(l-y) + v_l(y-f)}{l-f} , \tag{56}$$

which shows that v_1 and v_2 will vary linearly with y. Using Eqs. (56) and taking the values of df/dx, dV_0/dx and dv_l/dx as zero, Eqs. (47), (48) and (49) are transformed as follows,

$$\begin{aligned} g(Y_1 - Y_f) &= U_1 \frac{dv_f}{dx}\frac{f^2-y^2}{2f} + \left\{(v_f - V_0)\frac{f^2-y^2}{2f} + V_0(f-y)\right\}\frac{v_f - V_0}{f} , \\ -g(Y_2 - Y_f) &= U_2 \frac{dv_f}{dx}\frac{2l(y-f) - (y^2-f^2)}{2(l-f)} - [v_f\{2l(y-f) - (y^2-f^2)\} + v_l(y-f)^2] \\ &\quad \times \frac{v_f - v_l}{2(l-f)^2} , \end{aligned} \tag{57}$$

$$2g(Y_f - Y_l) = U_2 \frac{dv_f}{dx}(l-f) - (v_f^2 - v_l^2) \tag{58}$$

and

$$\begin{aligned} g(\overline{Y}_1 - Y_f) &= U_1 \frac{dv_f}{dx}\frac{f}{3} + (v_f - V_0)\left(\frac{v_f}{3} + \frac{V_0}{6}\right) , \\ -g(\overline{Y}_2 - Y_f) &= U_2 \frac{dv_f}{dx}\frac{l-f}{3} - (v_f - v_l)\left(\frac{v_f}{3} + \frac{v_l}{6}\right) . \end{aligned} \tag{59}$$

Here, a new notation Y is used instead of p in accordance with Eq. (18) in which

p_i' is taken constant in the same way as in the preceding article. $\overline{Y}_1$ and $\overline{Y}_2$, on the other hand, are related with U_1 and U_2 by

$$\overline{Y}_1 = \overline{Y}_{1,0} - \frac{U_1^2}{g} \quad \text{and} \quad \overline{Y}_2 = \overline{Y}_{2,0} - \frac{U_2^2}{g}, \tag{60}$$

which are the integrated forms of Eqs. (46) under the conditions $df/dx=0$ and $\overline{Y}_1=\overline{Y}_{1,0}$, $\overline{Y}_2=\overline{Y}_{2,0}$ and $U_1=U_2=0$ when $x=0$ and $\alpha_m=1$. Moreover, Eq. (19) may be used instead of Eq. (7).

Introducing Eqs. (59) into Eqs. (60) and considering the boundary conditions at $x=0$ noted above, the elimination of Y_f from the result yields

$$2\{U_1 f + U_2(l-f)\}\frac{dv_f}{dx} + (v_0 - v_l)(v_{f,0} - v_f) = -6(U_1^2 - U_2^2), \tag{61}$$

in which $v_{f,0}=(v_f)_{x=0}$. Since U_1 and U_2 are expressed as the integrated forms of Eqs. (55)

$$U_1 = \frac{1}{f}\left(V_0 x - \int_0^x v_f dx\right) \quad \text{and} \quad U_2 = \frac{1}{l-f}\left(\int_0^x v_f dx - v_l x\right), \tag{62}$$

Eq. (63), concerning v_f, is derived from Eq. (61)

$$\begin{aligned} &2f^2(l-f)^2\frac{dv_f}{dx}(V_0 - v_l)x - f^2(l-f)^2(V_0 - v_l)(v_f - v_{f,0}) \\ &= 6\left[-l(l-2f)\left(\int_0^x v_f dx\right)^2 + 2\{V_0(l-f)^2 - v_l f^2\}x\int_0^x v_f dx - \{V_0^2(l-f)^2 - v_l^2 f^2\}x^2\right]. \end{aligned} \tag{63}$$

Here, the dimensionless factors, λ and ξ, defined by Eqs. (23) are used again and the ratio of f to l is written as

$$f/l = \varphi. \tag{64}$$

As the equation of continuity applied to the whole domain of the inlet chamber, the relation

$$V_0 D = \int_0^B v_f dx = v_l B, \tag{65}$$

is identified, by which the ratio w is defined as

$$V_0/v_l = B/D = w. \tag{66}$$

Each value of φ, between zero and unity, corresponds to each point on the boundary of the counter and regular flow zones, and w, the ratio of the inlet opening to the total length of the basin, is usually larger than unity. Also, another ratio, r_f, relative to v_f, is introduced in the same way as Eq. (22), that is

$$v_f B \Big/ \int_0^B v_f dx = v_f/v_l = r_f, \tag{67}$$

and finally the dimensionless expression of Eq. (63) becomes

$$\frac{d^2s_f}{d\xi^2}=\frac{1}{2\xi}\left(\frac{ds_f}{d\xi}-r_{f,0}\right)-\frac{3(1-2\varphi)}{\lambda^2\varphi^2(1-\varphi)^2(w-1)\xi}\left\{s_f-\frac{w(1-\varphi)-\varphi}{1-2\varphi}\xi\right\}[s_f-\{w(1-\varphi)+\varphi\}\xi], \tag{68}$$

in which $r_{f,0}=(r_f)_{\xi=0}=v_{f,0}/v_l$ and $s_f=\int_0^\xi r_f d\xi$.

To solve Eq. (68) rigorously, numerical integration which starts at the boundary values $r_f=r_{f,0}$, $s_f=0$ and $dr_f/d\xi=0$* at $\xi=0$ is still necessary, and those difficulties in the process of obtaining a solution due to the existence of the two intercepting side walls still remained. Therefore, a further approximation must be made to represent the solution of Eq. (68) as a function of $r_{f,0}$.

If r_f is taken as constant, $r_{f,0}$, then $d^2s_f/d\xi^2=0$ and $s_f=r_f\xi$, in the region $0\leqq\xi\leqq 1/w\,(0\leqq x\leqq D)$ therefore, substituting these relations into Eq. (68) yields two independent solutions:—

$$r_f=\{w(1-\varphi)-\varphi\}/(1-2\varphi), \tag{69}$$

or

$$r_f=w(1-\varphi)+\varphi. \tag{69}'$$

After converting r_f of Eq. (69)′ into v_f and calculating the values of v, U_1 and U_2 by Eqs. (56) and (62), it appears that v varies linearly from V_0 to v_l transversally across the chamber, and that both U_1 and U_2 become independent of φ and equal to $(V_0-v_l)\xi/\lambda$ which always takes a positive value, so there is no clear distinction between the counter and regular flow zones. According to these facts it seems that solution (69)′ is not utilized conveniently for the flow under consideration. On the contrary, solution (69) gives $U_1=-U_2=-(V_0-v_l)\xi/\lambda(1-2\varphi)$, so, if φ is less than 1/2, U_1 takes a negative value and also $v_f>V_0$. In another words, there seem to be two adjacent, mutually counter-flowing zones. With the results of the above investigations, r_f is assumed to be expressed in the form

$$r_f=\{w(1-\varphi)-\varphi\}/(1-2\varphi)+\Delta r_f, \tag{70}$$

which is substituted into Eq. (68) with the term $\left(\int_0^\xi \Delta r_f d\xi\right)^2$ being ignored as an approximation, yielding

$$-\frac{\lambda^2\varphi(1-\varphi)}{6}\frac{d\Delta r_f}{d\xi}+\frac{\lambda^2\varphi(1-\varphi)}{12}\frac{\Delta r_f-\Delta r_{f,0}}{\xi}=\int_0^\xi \Delta r_f d\xi, \tag{71}$$

where $\Delta r_{f,0}=r_{f,0}-\{w(1-\varphi)-\varphi\}/(1-2\varphi)$. The solution of Eq. (71) is obtained considering the condition $\Delta r_f=\Delta r_{f,0}$ and $d\Delta r_f/d\xi=dr_f/d\xi=0$ at $\xi=0$, for which Δr_f is converted into r_f. Finally

---

* This can be obtained, by combining Eqs. (59) and (60) after differentiation, then substituting Eqs. (55) and $x=0$, $U_1=U_2=0$.

$$r_f = r_{f,0} + \left\{ r_{f,0} - \frac{w(1-\varphi)-\varphi}{1-2\varphi} \right\} F_{2m-1}(K\xi^2) ,$$

$$\frac{d r_f}{d\xi} = \left\{ r_{f,0} - \frac{w(1-\varphi)-\varphi}{1-2\varphi} \right\} F_{2m}(K\xi^2) \frac{1}{\xi} , \tag{72}$$

$$\int_0^\xi r_f d\xi = r_{f,0}\xi + \left\{ r_{f,0} - \frac{w(1-\varphi)-\varphi}{1-2\varphi} \right\} F_{2m+1}(K\xi^2)\xi ,$$

where
$$K = 12/\lambda^2\varphi(1-\varphi) , \tag{73}$$

and

$$F_{2m-1}(t) = \sum_{m=1}^{\infty} \{(-1)^m t^m / 1\cdot3\cdot5\cdot\cdots\cdot(2m-1)\cdot3\cdot7\cdot11\cdot\cdots\cdot(4m-1)\} ,$$

$$F_{2m}(t) = \sum_{m=1}^{\infty} \{(-1)^m 2mt^m / 1\cdot3\cdot5\cdot\cdots\cdot(2m-1)\cdot3\cdot7\cdot11\cdot\cdots\cdot(4m-1)\} , \tag{74}$$

$$E_{2m+1}(t) = \sum_{m=1}^{\infty} \{(-1)^m t^m / 1\cdot3\cdot5\cdot\cdots\cdot(2m-1)(2m+1)\cdot3\cdot7\cdot11\cdot\cdots\cdot(4m-1)\} .$$

are obtained.

In the same manner as above, those relations required for the region $1/w \leqq \xi \leqq 1$ $(D \leqq x \leqq B)$ are written as follows, corresponding to Eq, (72).

$$r_f = r_{f,B} + \left(r_{f,B} + \frac{\varphi}{1-2\varphi} \right) F_{2m-1}\{K(1-\xi)^2\} ,$$

$$\frac{d r_f}{d\xi} = -\left(r_{f,B} + \frac{\varphi}{1-2\varphi} \right) F_{2m}\{K(1-\xi)^2\} \frac{1}{1-\xi} , \tag{72}'$$

$$\int_1^\xi r_f \, d\xi = -r_{f,B}(1-\xi) - \left(r_{f,B} + \frac{\varphi}{1-2\varphi} \right) F_{2m+1}\{K(1-\xi)^2\}(1-\xi) .$$

Due to the relatively large value of K in Eq. (73), the infinite alternate series in Eqs. (74) converges slowly, and when ξ becomes larger, scores of terms are actually required. However, it is possible to present graphs which will serve conveniently for the computation. $F_{2m-1}(t)$, $F_{2m}(t)$ and $F_{2m+1}(t)$ are all oscillating functions varying from the mean value, -1, and their periods increase as t increases. Amplitudes of the former two functions also increase with the increase of t, whereas the third takes a relatively smaller amplitude than the former two which reduces still further as t increases. Hence, $\int_0^\xi \Delta r_f d\xi$ is supposed to take small enough values compared with Δr_f and $d\Delta r_f/d\xi$ except at the points where $F_{2m-1}(K\xi^2) = -1$ or $F_{2m}(K\xi^2) = 0$, so that the term $\left(\int_0^\xi \Delta r_f d\xi \right)^2$ may be neglected while solving Eq. (68). Further discussions concerning the restrictions in applying solutions (72) and (72)′ are possible, but omitted here.

To calculate r_f and others by Eqs. (72) nnd (72)′, $r_{f,0}$, $r_{f,B}$ and φ must be decided at first; Eqs. (51), (52) and (54), which represent the conditions at the boundary of the inlet and the distributing zone, serve this purpose.

Since the conditions at the two side walls have already been satisfied, Eq. (65)

must be equivalent to Eqs. (51), so a new expression of Eq. (65) is used instead of Eqs. (51):

$$\int_0^1 r_f \, d\xi = 1 . \tag{75}$$

Using Eqs. (72) and (72)′, Eq. (75) becomes

$$\left\{1+F_{2m+1}\left(\frac{K}{w^2}\right)\right\} r_{f,0} + (w-1)\left[1+F_{2m+1}\left\{K\frac{(w-1)^2}{w^2}\right\}\right] r_{f,B}$$
$$= \frac{w(1-\varphi)-\varphi}{1-2\varphi} F_{2m+1}\left(\frac{K}{w^2}\right) - \frac{(w-1)\varphi}{1-2\varphi} F_{2m+1}\left\{K\frac{(w-1)^2}{w^2}\right\} + w . \tag{76}$$

Next, introducing Eqs. (51) and (52) into the equations of motion (60) and into the corresponding equations for the distributing zone, reduce to

$$\overline{Y}_{1,0} = \overline{Y}_{1,B} \qquad \text{and} \qquad \overline{Y}_{2,0} = \overline{Y}_{2,B} . \tag{77}$$

With Eqs. (77), Eqs. (59) and the corresponding equations for the distributing zone, the following relation is found after some mathematical operations:

$$w^2 + (w-1) r_{f,0} + r_{f,B} = 0 . \tag{78}$$

Then finally, considering that Eqs. (51) and (52) have already been satisfied, $x=D$ is substituted into Eqs. (59) and also in to the corresponding equations for the distributing zone, to yield

$$\begin{aligned} 6g(\overline{Y}_1)_{x=D} &= 6g(Y_{f,i})_{x=D} + \left\{2U_1 f \frac{d v_{f,i}}{dx} + (v_{f,i}-V_0)(2v_{f,i}+V_0)\right\}_{x=D} \\ &= 6g(Y_{f,d})_{x=D} + \left\{2U_1 f \frac{d v_{f,d}}{dx} + 2v_{f,d}^2\right\}_{x=D} , \\ 6g(\overline{Y}_2)_{x=D} &= 6g(Y_{f,i})_{x=D} - \left\{2U_2 (l-f) \frac{d v_{f,i}}{dx} - (v_{f,i}-v_l)(2v_{f,i}+v_l)\right\}_{x=D} \\ &= 6g(Y_{f,d})_{x=D} - \left\{2U_2 (l-f) \frac{d v_{f,d}}{dx} - (v_{f,d}-v_l)(2v_{f,d}+v_l)\right\}_{x=D} . \end{aligned} \tag{*}$$

These equations are combined after $(Y_{f,i})_{x=D} = (Y_{f,d})_{x=D}$ in accordance with Eq. (54) and $(U_1)_{x=D}$, $(U_2)_{x=D}$ is calculated by Eqs. (62); consequently, the following relationship is derived.

$$2\left\{\left(\frac{d r_{f,i}}{d\xi}\right)_{\xi=1/w} - \left(\frac{d r_{f,d}}{d\xi}\right)_{\xi=1/w}\right\}\frac{w-1}{w} = w^2 + (w-1)(r_{f,i})_{\xi=1/w} + (r_{f,d})_{\xi=1/w} . \tag{79}$$

The practical steps for finding the required combination ($r_{f,0}$, $r_{f,B}$ and φ) are: (i) φ is first assumed, and then Eqs. (76) and (78) are solved together to find $r_{f,0}$ and $r_{f,B}$; (ii) the values of $r_{f,i}$, $r_{f,d}$, $d r_{f,i}/d\xi$ and $d r_{f,d}/d\xi$ at $\xi = 1/w$ are found

* Eq. (78) can also be derived from these equations by eliminating $(Y_{f,i})_{x=D} - (Y_{f,d})_{x=D}$ and using $(dv_{f,i}/dx)_{x=D}$ and $(dv_{f,d}/dx)_{x=D}$ obtained in Eq. (63).

by Eqs. (72) and (72)′; (iii) the assumption of value for φ and the above operations are repeated so as yield values which satisfy Eq. (79). There must be at least two combinations of ($r_{f,0}$, $r_{f,B}$ and φ) which satisfy the conditions, but since any combination including $\varphi>1/2$ is improper because it makes $U_1>0$ and $U_2<0$, the combination of $\varphi<1/2$ must be chosen.

After r_f, the relative value of v_f is determined by the method above mentioned, and all of the values U_1, U_2, Y_1, Y_2, Y_f, Y_l, etc. can be determined. The purpose of the analysis, however, is to find the appropriate ratio of opening along the diffuser wall to produce uniform diffusion of flow through the wall. These procedures are explained as follows:

Transformation of Eq. (58), after substitution of Eq. (19), leads to

$$\frac{2gY_f}{v_l^2}=2\varepsilon^*+\lambda(1-\varphi)q_2\frac{dr_f}{d\xi}+1-r_f^2, \tag{80}$$

where ε^* represents the required local value of ε which satisfies the above noted condition, and q_2 denotes U_2/v_l. Let ε_0^* signify the value of ε^* at $\xi=0$ and consider the boundary conditions at $\xi=0$, Eq. (80) becomes

$$\frac{2gY_{f,0}}{v_l^2}=2\varepsilon_0^*+1-r_{f,0}^2.$$

Hence, using the second equation of Eqs. (59), the value of $\overline{Y}_{2,0}$ is determined by

$$\frac{2g\overline{Y}_{2,0}}{v_l^2}=2\varepsilon_0^*-\frac{1}{3}r_{f,0}(r_{f,0}+1)+\frac{2}{3}.$$

Combination of the second equations of both (59) and (60), and introduction of $\overline{Y}_{2,0}$ above, results in

$$\frac{2gY_f}{v_l^2}=2\varepsilon_0^*-\frac{1}{3}r_{f,0}(r_{f,0}+1)+\frac{2}{3}-2q_2^2+\frac{2}{3}\lambda(1-\varphi)q_2\frac{dr_f}{d\xi}-2(r_f-1)\left(\frac{r_f}{3}+\frac{1}{6}\right).$$

When this Y_f is equated with Eq. (80), the final relation is obtained.

$$2\varepsilon^*=2\varepsilon_0^*-\frac{1}{3}r_{f,0}(r_{f,0}+1)+\frac{1}{3}r_f(r_f+1)-2q_2^2-\frac{1}{3}\lambda(1-\varphi)q_2\frac{dr_f}{d\xi}. \tag{81}$$

Distribution of Y_l may be calculated by Eq. (19) using ε^* of Eq. (81) and the fluctuation of values of e^* is also checked by $e^*=1/c\sqrt{2\varepsilon^*}$ when the magnitude of c at the orifice is given. Eq. (81) was derived only by the relationships for the inlet zone ($0\leqq x\leqq D$), but may still be available for the entire reach $x=0$ to B because U_2 and $\overline{Y}_2$ were treated as continuous at $x=D$, and the second equation of (59) also takes quite the same form for the distributing zone. It must be noted, however, that $(\varepsilon_l^*)_{x=D}$ and $(\varepsilon_d^*)_{x=D}$ are obtained separately since

the values of r_f and $dr_f/d\xi$ might not always be continuous at $x=D$, and that errors due to those approximate calculations may inevitably accumulate in the counter flow zone by reason of the fact that only the equation of motion for the regular flow zone was used in the process of getting Eq. (81). The latter fact is assumed rather appropriate while investigating the immediate effect of the diffuser wall.

As seen from Eq. (81), if λ and w are given, the difference between ε^* and ε_0^* at any point on the diffuser wall takes a definite value regardless of the magnitude of ε_0^*. Accordingly, the larger the value of ε_0^* becomes, the smaller the ratio $(\varepsilon^*-\varepsilon_0^*)/\varepsilon_0^*$ may be. If the range of variations of ε^* or e^* is relatively narrow, the following approximate expression is adopted

$$r = \overline{e^*}/e^*, \tag{82}$$

where r denotes the relative uniformity of velocity v_l as defined in Eq. (22) when constant opening ratio $e=\overline{e^*}=\int_0^1 e^* d\xi$ over the wall is adopted. It is easily realized from Eq. (82) that uniform distribution of flow will be accomplished by using smaller openings in the wall. On the contrary, with large values of e_0^* which lead to negative values for the right side in Eq. (81), it is impossible to distribute the flow uniformly. Hence e_0^* must satisfy the next relation:

$$2\varepsilon_0^* > \left\{\frac{1}{3} r_{f,0}(r_{f,0}+1) - \frac{1}{3} r_f(r_f+1) + 2q_2^2 + \frac{1}{3}\lambda(1-\varphi)q_2 \frac{dr_f}{d\xi}\right\}_{\max}. \tag{83}$$

—— Numerical Example and Discussions ——

Now, an example of the numerical calculation by the above described method for $\lambda=1/3$ and $w=3$ will be shown as follows. The values of φ, $r_{f,0}$ and $r_{f,B}$ determined by Eqs. (76), (78) and (79) are 0.210, -2.657 and -3.686 respectively. Fig. 11

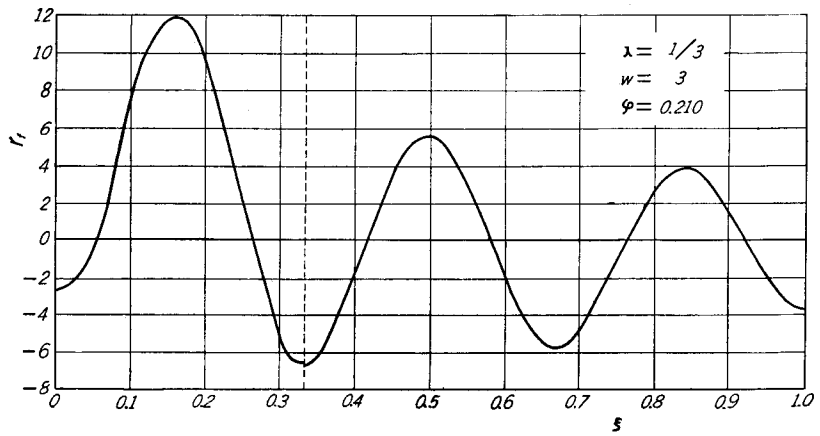

Fig. 11. Lateral velocity distribution on the boundary of counter and regular flow zones.

shows the varition of r_f and Fig. 12 that of $q_1(=U_1/v_l)$ and q_2. The flow pattern in the inlet chamber due to uniform diffusion through the wall becomes a definite one regardless of the number of openings in the wall as illustrated in Figs. 11 and 12.

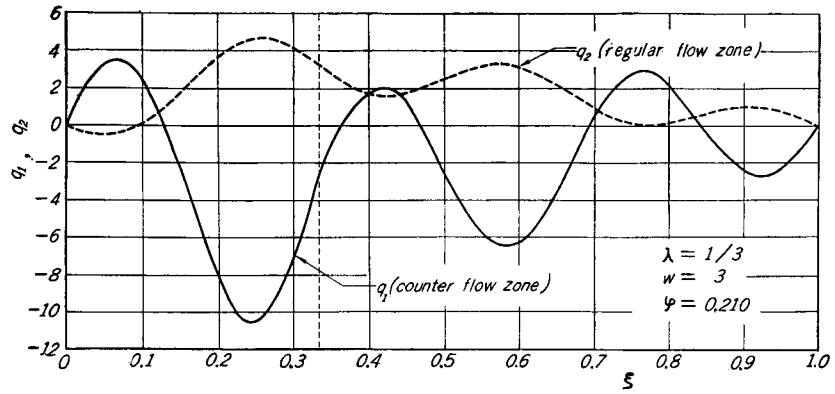

Fig. 12. Main flow behaviours in both zones.

With periodic change in the value of r_f, the values q_1 and q_2 also show similar variations, and particularly the flow in the counter flow zone partly alternates in its direction, whereas in the greater part of the regular flow zone it takes the positive direction of x. Since the mean value of r_f between $\xi=1/3$ and 1, however, is -0.282, U_1 becomes negative as a whole. On the other hand, between $\xi=0$ to 1/3 r_f averages to 3.565, although it varies a little more roughly, and exceeds the rate $V_0/v_l=w=3$ by 0.565 which corresponds to the scale of counter flow. Therefore, the existence of a large scale circulation covering the regular and counter flow zones, in addition to the small local ones, was now verified numerically. Let the ratio of flow circulating to the inflow from the inlet conduit be defined as the circulation ratio. It will be expressed as the integral of r_f and is calculated in this case as follows:

$$\text{circulation ratio} = \int_0^D v_f dx \Big/ V_0 D = \int_0^{1/w} r_f d\xi = 1.188. \tag{84}$$

It may be concluded that in order to obtatin evenly distributed flow along diffuser wall, perpendicular to the directian of the inlet conduit, the entering flow must be reflected at the diffuser wall, a part of which is circulated. These phenomena may be attributed to the action of the diffuser wall which maintains the actual velocity of the water fraction in the chamber to some extent, keeps the velocity terms in Eqs. (60) as unchanged as possible, and prevents the pressure from increasing, during which the whole inlet chamber plays the role of

cushion against the inflowing water.

Variations of ce^* according to various values of ce_0^* are illustrated in Fig. 13, which shows delicate changes similar to the variations of r_f, q_1 and q_2 in Figs. 11 and 12. As seen in Fig. 13, when $\lambda=1/3$, $w=3$, $c=1/\sqrt{1.5}$ and e is constant, a satisfactory distribution of flow will be expected for e less than about 8%,

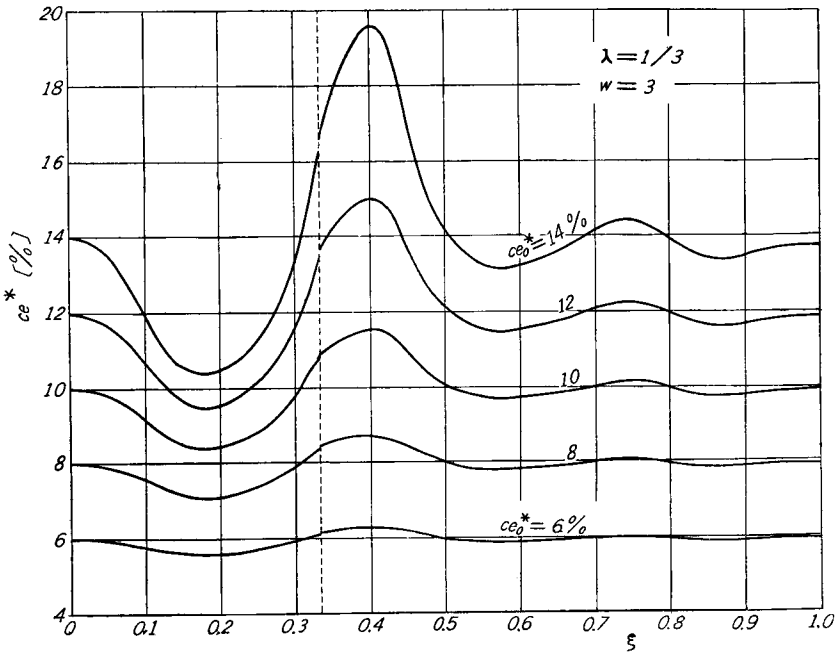

Fig. 13. Necessary change in opening ratio (referring to Fig. 9).

which seems applicable in actual practice. On the contrary, increasing the average opening ratio causes considerable change in its local value, especially, e^* takes a maximum value, which is due to the minimum of $2\varepsilon^*=2gY_l/v_l^2$ in the vicinity of $\xi=0.4$. Since $2\varepsilon_0^*-(2\varepsilon^*)_{\xi=0.4}=24.971$, the value of $2\varepsilon_0^*$ must be taken more than 24.971 or ce_0^* less than about 20%.

Again in Fig. 13, there is seen a constant difference between the maximum and minimum value of $2\varepsilon^*$ and the maximum value occurs near $\xi=0.18$, which is related as

$$\left(\frac{2gY_l}{v_l^2}\right)_{\max}-\left(\frac{2gY_l}{v_l^2}\right)_{\min}=68.260\,.$$

If 1 cm/sec is assumed as v_l in the actual basin, the difference $(Y_l)_{\max}-(Y_l)_{\min}$ is merely 0.035 cm. Accordingly, it may be assumed that Y, the water depth in the inlet chamber, will readily fluctuate due to the influence of poor or mistaken

design of the openings in the wall or due to natural obstacles – for instance the existence of difference in water temperature or density and wind drift— so that, except for an ideal basin, the effects of the diffuser wall seems unstable. Hence, it is necessary to increase the magnitude of v_l and select a chamber of such form as to cause a larger variation of Y_l or e^* locally so as to diminish such obstacles. It must be noted, however, that the significance of the latter requirement is different from increasing the actual value of Y_l by adopting a lower value of e or e^*. Due to the increase of v_l, the Froude numbers in both the inlet chamber and the settling zone also increase. Also the circulation in the chamber results in the increase of the Froude number. According to Camp's proposal[5], the Froude number v_l^2/gH in the settling tank of the horizontal flow type must be raised up to the range $10^{-6}\sim10^{-4}$ for the purpose of improving the unstable flow and increasing the volumetric efficiency in the tank which have been conventionally designed with the above number set at 10^{-7}; the reliability of this proposal has been confirmed here again in view of the analysed flow behaviour through the inlet diffuser wall.

Finally, Fig. 14 illustrates the relative distribution of v_l, for the case of uniform perforation referring to Eq. (82) and Fig. 13. However, Eq. (82) is an approximate expression applicable only when the pressure distribution is close to that of $r\equiv1$, so that, if r fluctuates widely with the greater values of ce the

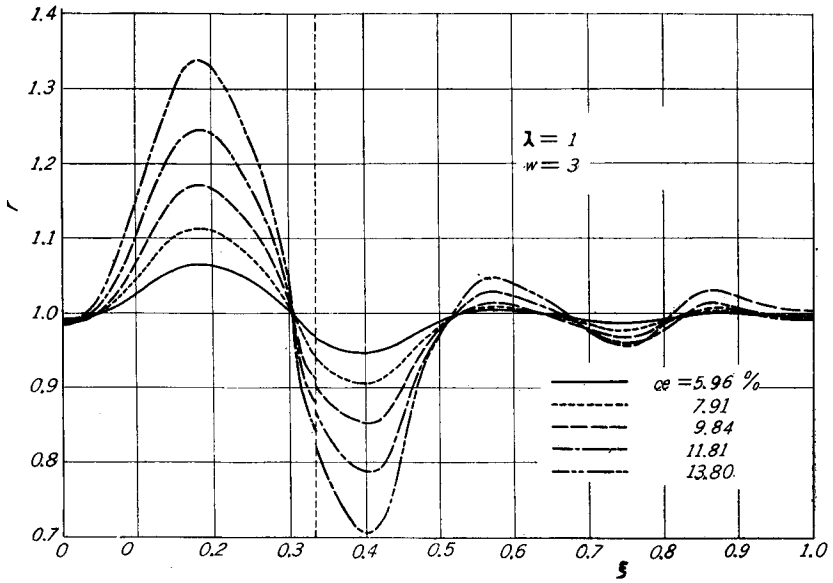

Fig. 14. Flow distribution through diffuser wall with constant perforation ratio (referring to Fig. 9).

values of r_f, q_1, q_2 and Y may differ from the case of uniform diffusion, and the values of r given in Fig. 14 will also be in error. As seen in Fig. 14, the occurrence of the maximum value of r in the inlet zone, which faces the inlet conduit directly, is generally expected, but it must also be noticed that r takes a rather low value at the section a little distant from the inlet zone, whereas it shows a relatively uniform distribution in the remaining part of the distributing zone.

5. Summary

In this paper, the flow behaviours in two-dimensionalized inlet chambers were discussed theoretically in order to make clear the flow-distributing mechanism of the inlet diffuser wall in settling tanks. Such an attempt has not been made previously. The method and results may be summarized as follows:

In the fundamental consideration:—

(i) the two-dimensional flow in the belt-shaped zone was analysed by the one-dimensional method considering the lateral component of flow along the boundaries as the in- and out-flow, and the basic theoretical relationships were introduced neglecting the effect of the viscosity of the fluid.

For the rectangular inlet chamber with an inlet conduit perpenicular to the basin axis:—

(ii) in most cases, the velocity v_l through the wall can be expressed by the same formula (36) as the one which is obtained for the outflow distribution from the uniformly perforated pipe, but in this case a definite lateral profile of the water surface is seen in the chamber.

(iii) Near the entrance section of the inlet conduit, however, there exists a transitional region to some extent, the length of which increases when the width of the chamber is shorter or the degree of perforation of the diffuser wall increases.

(iv) In case the diffuser wall is uniformly perforated, the flow will turn aside towards the far end side wall of the basin, and that tendency increases when the transition region spreads further in the same manner as (iii), so that, the local opening ratio of the wall nearer to the inlet junction must be much larger if the ideal distribution of flow is required.

For the rectangular inlet chamber with an inlet conduit perpendicular to the diffuser wall:—

(v) based on the hydraulic characteristics, the chamber would be appropriately divided into two parts: "counter flow zone" and "regular flow zone".

(vi) If the problem is confined to the case of uniform diffusion through the diffuser, the approximate solution of Eq. (68), related to the lateral velocity component v_f on the boundary of both zones, yields Eqs. (72) and (72)', by which

the flow pattern and the required changing rate of opening along the diffuser wall are computed.

(vii) The results of numerical calculation for the inlet chamber connected to the inlet conduit of 1/3 width actually verified that the flow circulates in the chamber at a circulation ratio of about 1.2 and indicated that the local rate of perforation to attain the uniform distribution of flow must be adjusted delicately as shown in Fig. 13.

(viii) Inasmuch as the local change of water depth is supposed insignificant in the actual chamber, it will be necessary to raise the absolute value of v_l on account of establishing the stable effect of the diffuser wall.

(ix) When an uniform opening rate through the entire wall is adopted, it will cause an unforeseen low value of v_l at the section a short distance from the front of the inlet.

Although those analyses were limited to two typical cases of the inlet chamber, the characteristics of flow in the chamber shown in Fig. 1 (b) are also capable of analysis by a similar method to that described in this paper. Also, though only one numerical example was introduced for the case of Fig. 10, application of the results for Fig. 4 and further theoretical treatment utilizing Eqs. (69), (69)′, (72) and (72)′ may possibly reduce the theoretically based prediction for the effect of inlet devices of various geometric proportions in Fig. 10. Since the structural differences (whether perforated or slotted vertical) in the diffuser wall may only contribute to changes in the discharge coefficient c in Eq. (7), the above treatise will be applicable to both cases.

The results of detailed experiments will be published soon.

Acknowledgement

This paper is part of the research project "hydraulics of water collection and distribution in water supply and sewerage" financially supported by the Ministry of Education.

Bibliography

1) T. Sueishi; Kogyo-Yosui, No. 17, 6 (1960).
2) H. Wiegmann and Müller-Neuhaus; Die Wasserwirtsch. (1950).
3) G. E. Mau; Sewage and Industrial Waste, **31**, 1349 (1959).
4) T. Goda; Trans. JSCE, **4**, 69 (1949).
5) T. R. Camp; Trans. ASCE, **111**, 895 (1946).